Characterization of NO_x, SO_2, ethene, and propene from industrial emission sources in Houston, Texas

R. A. Washenfelder,[1,2] M. Trainer,[2] G. J. Frost,[1,2] T. B. Ryerson,[2] E. L. Atlas,[3] J. A. de Gouw,[1,2] F. M. Flocke,[4] A. Fried,[4] J. S. Holloway,[1,2] D. D. Parrish,[2] J. Peischl,[1,2] D. Richter,[4] S. M. Schauffler,[4] J. G. Walega,[4] C. Warneke,[1,2] P. Weibring,[4] and W. Zheng[4]

Received 2 December 2009; revised 19 April 2010; accepted 28 April 2010; published 28 August 2010.

[1] The Houston-Galveston-Brazoria urban area contains industrial petrochemical sources that emit volatile organic compounds and nitrogen oxides, resulting in rapid and efficient ozone production downwind. During September to October 2006, the NOAA WP-3D aircraft conducted research flights as part of the second Texas Air Quality Study (TexAQS II). We use measurements of NO_x, SO_2, and speciated hydrocarbons from industrial sources in Houston to derive source emission ratios and compare these to emission inventories and the first Texas Air Quality Study (TexAQS) in 2000. Between 2000 and 2006, NO_x/CO_2 emission ratios changed by an average of −29% ± 20%, while a significant trend in SO_2/CO_2 emission ratios was not observed. We find that high hydrocarbon emissions are routine for the isolated petrochemical facilities. Ethene (C_2H_4) and propene (C_3H_6) are the major contributors to ozone formation based on calculations of OH reactivity for organic species including C_2–C_{10} alkanes, C_2–C_5 alkenes, ethyne, and C_2–C_5 aldehydes and ketones. Measured ratios of C_2H_4/NO_x and C_3H_6/NO_x exceed emission inventory values by factors of 1.4–20 and 1–24, respectively. We examine trends in C_2H_4/NO_x and C_3H_6/NO_x ratios between 2000 and 2006 for the isolated petrochemical sources and estimate a change of −30% ± 30%, with significant day-to-day and within-plume variability. Median ambient mixing ratios of ethene and propene in Houston show decreases of −52% and −48%, respectively, between 2000 and 2006. The formaldehyde, acetaldehyde, and peroxyacetyl nitrate products produced by alkene oxidation are observed downwind, and their time evolution is consistent with the rapid photochemistry that also produces ozone.

Citation: Washenfelder, R. A., et al. (2010), Characterization of NO_x, SO_2, ethene, and propene from industrial emission sources in Houston, Texas, *J. Geophys. Res.*, *115*, D16311, doi:10.1029/2009JD013645.

1. Introduction

[2] Ozone (O_3) is the most abundant oxidant in the troposphere and can be considered a principal product of tropospheric chemistry. It is formed by photochemical reactions involving nitrogen oxides (NO_x) and reactive volatile organic compounds (VOCs) [*Haagen-Smit*, 1952; *Crutzen*, 1979]. Reduction of NO_x and VOC emissions under the U. S. Clean Air Act of 1970 and its subsequent amendments has been partially successful in reducing ozone concentrations within the United States, but understanding and predicting exceedances remain a challenge.

[3] During daytime conditions, VOCs react primarily with hydroxyl radicals (OH). The resulting peroxy radicals can react with nitric oxide (NO) to regenerate OH and form nitrogen dioxide (NO_2). The rate and efficiency of ozone production depends on the absolute concentrations of NO_x and VOCs, as well as the ratio of these species. Ambient measurements have confirmed that the rate and magnitude of ozone production differs for plumes downwind of different anthropogenic source types characterized by different NO_x and VOC emission ratios [e.g., *Gillani et al.*, 1998; *Ryerson et al.*, 1998; *Daum et al.*, 2000; *Ryerson et al.*, 2001, 2003]. The fastest rate of ozone formation and highest yields per NO_x molecule emitted are predicted for conditions where elevated concentrations of NO_x and reactive VOCs are simultaneously present.

[4] The city of Houston, Texas, is the fourth largest in the United States, and the greater Houston urban area is home to

[1]Cooperative Institute for Research in Environmental Sciences, University of Colorado, Boulder, Colorado, USA.
[2]Chemical Sciences Division, Earth System Research Laboratory, National Oceanic and Atmospheric Administration, Boulder, Colorado, USA.
[3]Division of Marine and Atmospheric Chemistry, University of Miami, Miami, Florida, USA.
[4]Earth Observing Laboratory, National Center for Atmospheric Research, Boulder, Colorado, USA.

0148-0227/10/2009JD013645

Table 1. Relevant Measurements Acquired Onboard the NOAA WP-3D Aircraft During TexAQS 2006

Species	Technique	Uncertainty (1σ)	Frequency	Reference
O_3	Chemiluminescence	±(0.050 ppbv + 3%)	1 Hz	[*Ryerson et al.*, 1999, 2000]
NO	Chemiluminescence	±(0.015 ppbv + 5%)	1 Hz	[*Ryerson et al.*, 1999, 2000]
NO_2	Photolysis to NO with chemiluminescence	±(0.040 ppbv + 9%)	1 Hz	[*Ryerson et al.*, 1999, 2000]
NO_y	Thermal conversion to NO with chemiluminescence	±(0.20 ppbv + 12%)	1 Hz	[*Ryerson et al.*, 1999, 2000]
CO	Vacuum UV fluorescence	±(1.0 ppbv + 5%)	1 Hz	[*Holloway et al.*, 2000]
CO_2	Nondispersive IR absorption	±0.12 ppmv	1 Hz	[*Peischl et al.*, 2010]
SO_2	UV pulsed fluorescence	±(0.3 ppbv + 10%)	1 Hz	[*Ryerson et al.*, 1998]
CH_2O	Difference frequency generation absorption spectroscopy	±(0.12 ppbv + 6.5%)	1 Hz	[*Weibring et al.*, 2007]
PANs	Thermal decomposition–chemical ionization mass spectrometry	±30%	1 Hz	[*Slusher et al.*, 2004]
C_2H_4	Laser photoacoustic spectroscopy	±(0.7 ppbv + 20%)	0.05 Hz	[*de Gouw et al.*, 2009]
Speciated VOCs	Whole air samples analyzed by gas chromatography	5%–10%	80/flight	[*Schauffler et al.*, 1999, 2003]
Speciated VOCs	Proton transfer reaction mass spectrometry	10%–20%	0.08 Hz	[*de Gouw et al.*, 2003]

more than five million people [*U. S. Census Bureau*, 2006]. Since 2004, Houston-Galveston-Brazoria has been designated as a nonattainment area under the 1997 National Ambient Air Quality Standards (NAAQS) for ozone. The stricter 2008 NAAQS rules require that the 3 year average of the fourth highest daily maximum 8 h average ozone concentrations measured at each monitoring site within an area over each year must not exceed 0.075 ppm. The high ozone levels in Houston are attributed to anthropogenic NO_x and VOC sources that combine to form ozone during periods of intense solar radiation and stagnant meteorological conditions. In addition to the typical urban emission sources, such as motor vehicles, the greater Houston area is home to the largest grouping of petrochemical industrial sources in the United States. However, the problems of petrochemical VOC emissions are not unique to Houston. Many cities contain industrial petrochemical sources, albeit on a smaller scale, and Houston serves as an important case study.

[5] In order to evaluate and predict air quality in the Houston area, it is important to understand the magnitude and variability of these industrial sources and how these sources are evolving over time. Previous studies in Houston reported high concentrations of VOCs that were not correctly included in emission inventories [*Kleinman et al.*, 2002; *Karl et al.*, 2003; *Ryerson et al.*, 2003; *Wert et al.*, 2003; *Jobson et al.*, 2004; *de Gouw et al.*, 2009; *Mellqvist et al.*, 2010]. Although concentrations of all measured VOCs exceeded values in emission inventories, the reactivity was dominated by a limited subset of highly reactive VOCs that included ethene and propene [*Ryerson et al.*, 2003; *Wert et al.*, 2003]. The high ozone concentrations observed in Houston were attributed to the presence of these highly reactive VOCs in a NO_x-rich atmosphere. Biogenic sources of VOCs also exist in and around Houston, although detailed vegetation surveys [*Wiedinmyer et al.*, 2001], aircraft measurements [*Wert et al.*, 2003], and ship-based measurements [*Gilman et al.*, 2009] indicate that these emissions are less important for ozone formation than those from anthropogenic sources near the Houston Ship Channel.

[6] One of the primary goals of the second Texas Air Quality Study (TexAQS II) in 2006 was to continue the work begun during the TexAQS 2000 study to improve understanding of the chemical and meteorological causes of ozone exceedance episodes in the Houston-Galveston-Brazoria and Dallas metropolitan areas. A second important goal was to evaluate potential changes in ozone precursor emissions between 2000 and 2006. During September to October 2006, measurements of gas phase species and particles were made by the NOAA WP-3D aircraft in plumes from power plant, petrochemical, and urban sources in Texas and neighboring states. Further description of the scientific goals and logistics of the TexAQS 2006 field campaign can be found in the work of *Parrish et al.* [2009].

[7] This work focuses on the emissions of NO_x, sulfur dioxide (SO_2), and VOCs from industrial sources in Houston, Texas. We examine trends in NO_x and SO_2 emissions between 2000 and 2006 for industrial sources. Using relative OH reactivity, we identify the highly reactive VOCs that are likely to contribute to ozone formation. We then present emission trends for ethene and propene between 2000 and 2006. Finally, we examine the photochemical oxidation products measured in downwind transects from industrial sources.

2. Experimental

2.1. Overview of TexAQS Field Measurements

[8] During the TexAQS 2006 study, the NOAA WP-3D was based at Ellington Field in Houston, Texas. The aircraft conducted 18 research flights between 31 August and 13 October 2006 in eastern Texas. Each research flight was approximately 6 h in duration. The flights focused on measurements of anthropogenic pollution during active photochemical periods, including downwind of urban areas, power plants, and petrochemical industrial facilities in the greater Houston area. Most data were acquired within the planetary boundary layer during daytime, with typical flight altitudes of 500 m above sea level for the plume transect measurements presented here. Plume transects were sampled by flying perpendicular to the prevailing wind direction under conditions when emissions from industrial complexes could be individually distinguished.

[9] For the measurements used in this analysis, Table 1 summarizes the instrumental techniques, uncertainty, frequency, and references containing further details. The stated uncertainty in Table 1 includes both precision and accuracy. Instruments onboard the NOAA WP-3D included 1 Hz measurements of O_3, NO, NO_2, peroxyacyl nitrates (PANs), total reactive nitrogen (NO_y), carbon monoxide (CO), SO_2, and carbon dioxide (CO_2) [*Ryerson et al.*, 1998, 1999;

Holloway et al., 2000; *Ryerson et al.*, 2000; *Slusher et al.*, 2004; *Peischl et al.*, 2010]. In addition, several instruments measured VOCs. Formaldehyde (CH_2O) was measured at 1 Hz by difference frequency generation absorption spectroscopy [*Weibring et al.*, 2007]. Ethene (C_2H_4) was measured at 5 s resolution with laser photoacoustic spectroscopy (LPAS) [*de Gouw et al.*, 2009]. Speciated VOCs were measured by both proton transfer reaction mass spectrometry (PTR-MS) [*de Gouw and Warneke*, 2007] and gas chromatography (GC) of 80 whole air samples acquired during each flight [*Schauffler et al.*, 1999, 2003]. The PTR-MS measured a select set of VOCs, including acetaldehyde (CH_3CHO), acetic acid, acetone, acetonitrile, benzene, toluene, C_8 and C_9 aromatics, methyl ethyl ketone, methanol, isoprene and its oxidation products (methyl vinyl ketone and methacrolein), and the sum of monoterpenes. The whole air sample measurements were less frequent but included a much larger suite of speciated VOCs, including C_2–C_{10} alkanes, C_2–C_5 alkenes, ethyne, and C_2–C_5 aldehydes and ketones (see *Ryerson et al.* [2003] for a complete list), along with CO and methane (CH_4).

[10] During the TexAQS 2000 study, the National Center for Atmospheric Research L-188C Electra aircraft was used. This aircraft was similarly based at Ellington Field in Houston, Texas, and conducted research flights during 18 August to 13 September 2000. A NOAA WP-3D transit flight south of Houston in 2002 provided additional data to construct trends. Both of these data sets have been described in detail previously [*Ryerson et al.*, 2003]. The 2000, 2002, and 2006 aircraft campaigns used many of the same instruments, including O_3, NO, NO_2, NO_y, CO, SO_2, and whole air sampler, which minimizes measurement bias in the observed temporal trends.

2.2. Meteorological and Ancillary Data

[11] During the 2000, 2002, and 2006 field campaigns, aircraft instruments recorded wind speed, wind direction, ambient temperature, and other meteorological parameters. Meteorological and chemical measurements acquired during vertical profiles were used to determine information about boundary layer height and vertical mixing within and above the boundary layer. In addition, the Radar Wind Profiler Network measured vertical profiles of boundary layer winds at 6 Texas sites in 2000 [*Nielsen-Gammon et al.*, 2008] and 10 Texas sites in 2006 [*Parrish et al.*, 2009]. Vertical mixing and boundary layer height were determined for the sites closest to Houston, which were Ellington Field in 2000 and La Porte in 2006. Uncertainties in wind speed of ± 1 m s^{-1} and in boundary layer height of $\pm 10\%$ were previously estimated by comparing derived values from the various aircraft and ground-based data sets [*Ryerson et al.*, 2003].

2.3. Emission Inventories

[12] Emission estimates derived from measurements are compared here to Point Source Emissions Inventories (PSEI) for 1999 and 2006. The 1999 inventory was previously provided by the Texas Natural Resource Conservation Commission (as described in the work of *Ryerson et al.* [2003]), and the 2006 inventory was provided by the Texas Commission on Environmental Quality (TCEQ) (John Jolly, personal communication). These are more detailed versions of the standard inventories that are reported by TCEQ to the Environmental Protection Agency (EPA) for inclusion in the National Emissions Inventory (NEI) data base. In particular, these inventories contain speciated VOC emissions data. In 2006, the Houston-Galveston-Brazoria area contained 506 accounts, which represent individual facilities and sites. In order to obtain the most complete and accurate bottom-up emission inventory, the 2006 PSEI inventory used in this work has been updated to include more detailed information when possible. The updates are described below.

[13] 1. During 15 August to 15 September 2006, 86 accounts were asked to provide hourly emissions data at the level of a "path," which is a uniquely defined combination of account, process unit, and emission point. Hourly path emissions were reported for 6% of the total paths for these 86 facilities, representing about 1% of the total paths in the Houston-Galveston-Brazoria area. This information has been incorporated into the PSEI.

[14] 2. Continuous Emissions Monitoring System (CEMS) instruments are installed on 17 of the largest sources in the Houston-Galveston-Brazoria area to monitor NO_x, SO_2, and CO_2 emissions. We have updated the PSEI to include the average CEMS measurements reported by these sources during September to October 2006.

[15] The TCEQ PSEI includes NO_x, SO_2, CO, total VOC, $PM_{2.5}$, and PM_{10} for sources in Texas. Emissions of hundreds of individual VOC compounds were also reported in the 1999 and 2006 TCEQ PSEI. When examining specific time periods in our analysis, we have considered hourly averaged emissions data from CEMS and estimates provided by facility operators. The timing and nature of nonroutine emission events at many facilities were also reported to TCEQ and are considered in this study.

3. Results and Discussion

3.1. Emission Inventory and Predicted Trends

[16] Figure 1 shows NO_x and total VOC emissions from the TCEQ 2006 PSEI for the Houston-Galveston-Brazoria area, as described in section 2.3. The map shows a 160 km × 160 km area and indicates the major petrochemical industrial complexes, including the Houston Ship Channel, Mont Belvieu, Texas City, Chocolate Bayou, Freeport, and Sweeny. In the southeastern United States, ozone production downwind of power plants is typically most efficient in the presence of reactive biogenic hydrocarbons, such as isoprene [*Ryerson et al.*, 2001]. The colocation of major NO_x and VOC sources at the petrochemical industrial complexes shown in Figure 1 has been shown to lead to rapid downwind ozone formation [*Kleinman et al.*, 2002; *Daum et al.*, 2003; *Ryerson et al.*, 2003]. In contrast, coal- and gas-fired power plants, such as W. A. Parish, emit relatively minor amounts of VOCs, as shown for the emissions inventory in Figure 1 and confirmed by downwind measurements during the TexAQS 2006 field campaign. The inventory values and trends for the six industrial complexes are given in Table 2. The TCEQ PSEI indicates reductions in NO_x and SO_2 emissions between 1999 and 2006.

[17] Reported CEMS monitoring has been found to be consistent with both NO_x and SO_2 measurements by the

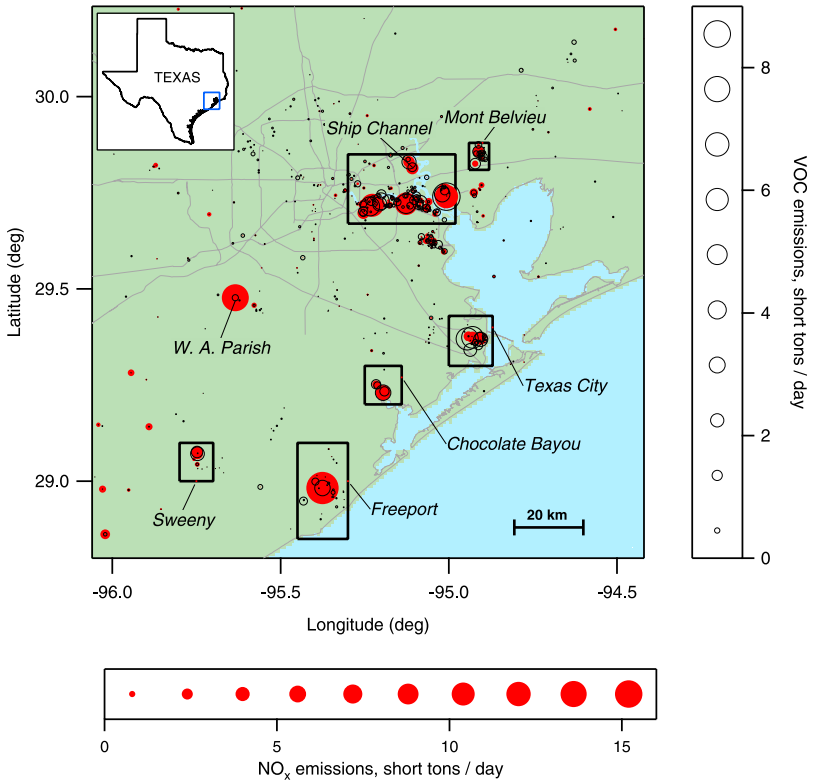

Figure 1. Map of emission sources near Houston, Texas, according to the Texas Commission on Environmental Quality's 2006 PSEI. Points are sized according to the magnitude of the emissions, with NO_x emissions shown as solid red circles and total volatile organic compound emissions shown as open black circles. The map labels six major petrochemical complexes. The location of the W. A. Parish power plant is also shown.

NOAA WP-3D aircraft [*Peischl et al.*, 2010]. Previous work has shown that NO_x controls on large power plants, such as W. A. Parish, have resulted in significant, measurable decreases in NO_x emissions. These reductions have been observed by the NOAA WP-3D [*Peischl et al.*, 2010] and satellite measurements [*Kim et al.*, 2006]. Some industrial sources in Houston have implemented NO_x and SO_2 controls, similar to the large power plants. These reductions may have led to the decreasing values for NO_x and SO_2 emissions in the TCEQ PSEI between 1999 and 2006, shown in Table 2.

3.2. Trends in NO_x and SO_2 Emissions for Industrial Sources

[18] Two different techniques are typically used to compare aircraft measurements to emission inventories. The first technique is the calculation of absolute fluxes [*White et al.*, 1976; *Trainer et al.*, 1995], which requires accurate knowledge of wind speed, wind direction, and aircraft speed. In addition, the boundary layer must be well defined and well mixed, and the emissions must have had sufficient time to mix vertically throughout the boundary layer. These are potential sources of error during meteorological conditions that do not have vigorous mixing or a well-defined boundary layer height or for aircraft transects that are close enough to the source that plumes have not had sufficient time to mix vertically. Poorly defined boundary layer heights and weak vertical mixing were observed during a number of the WP-3D flights in 2006. For this analysis, we have chosen to calculate emission ratios instead. This second method does not require knowledge of the boundary layer height or mixing and is not subject to the same assumptions and errors described above. Because emission ratios are determined from the enhancement of two species in a discrete plume, they are not sensitive to seasonal or meteorological changes that may affect the background concentration. Attribution of observed enhancement ratios to a single known source becomes complicated when multiple plumes coalesce. In this analysis, we have selected discrete plumes that exhibit enhanced mixing ratios for anthropogenic species and can be unambiguously matched to a source directly upwind.

[19] Figure 2a shows a time series of CO_2, NO_x, and SO_2 mixing ratios for one transect measured downwind of the Sweeny industrial complex. This particular transect was measured on 21 September 2006 10:37 local standard time at an altitude of 340 m. The plume was intersected 11.4 km from the source, after a transit time of approximately 0.3 h. Plume transit time is determined from the average wind speed at the time of the plume intersection and the distance from the source. Figures 2b and 2c show the NO_y/CO_2 and SO_2/CO_2 correlation plots for these data. The large measured ratio of NO_x/NO_y (97% ± 2%) shows that oxidation of NO_x was minimal, as expected from the short time between emission and measurement. Thus, losses of NO_y were minimal and NO_y measured downwind is a good proxy for

Table 2. TCEQ Point Source Emissions Inventory Values and Trends for 1999–2006 for the Industrial Areas Indicated in Figure 1[a]

	1999				
	NO_x	SO_2	C_2H_4	C_3H_6	VOCs
Houston Ship Channel	153.0	98.4	3.2	4.7	75.8
Mont Belvieu	9.2	3.1	1.6	0.3	5.1
Texas City	48.9	29.2	0.5	0.6	27.1
Chocolate Bayou	11.0	0.2	0.3	0.6	4.1
Freeport	54.1	6.7	0.7	0.4	5.2
Sweeny	17.4	22.1	0.1	0.1	4.4
W. A. Parish	90.4	185.2	0.0	0.0	0.5
	2006				
	NO_x	SO_2	C_2H_4	C_3H_6	VOCs
Houston Ship Channel	67.9	67.0	1.9	4.3	58.7
Mont Belvieu	5.0	0.6	2.2	1.0	8.5
Texas City	11.7	15.8	0.2	0.2	20.6
Chocolate Bayou	6.6	0.1	1.1	0.8	6.1
Freeport	24.3	7.7	1.2	0.3	5.8
Sweeny	7.5	4.4	0.3	0.2	4.4
W. A. Parish	14.5	167.1	0.0	0.0	0.5
	Percentage Change				
	NO_x	SO_2	C_2H_4	C_3H_6	VOCs
Houston Ship Channel	−56	−32	−41	−8	−23
Mont Belvieu	−46	−82	38	212	65
Texas City	−76	−46	−64	−61	−24
Chocolate Bayou	−40	−32	305	27	48
Freeport	−55	14	77	−33	11
Sweeny	−57	−80	151	53	0
W. A. Parish	−84	−10	0	0	13

[a]Values are reported in short tons d^{-1}, with NO_x reported as NO_2.

the direct emissions of NO_x. The fit in each case is determined from the linear orthogonal distance regression, weighted by the measurement imprecision (as given in Table 1). The industrial complexes contain multiple discrete units whose emissions typically cannot be separated in the WP-3D data. The slopes of the correlation plots for downwind transects are equal to the net emission ratios for the entire complex.

[20] Emission ratios of NO_x/CO_2 and SO_2/CO_2 were calculated for all WP-3D and Electra transects of Texas City, Sweeny, and Chocolate Bayou industrial plumes during 2000, 2002, and 2006 following the example shown in Figures 2b and 2c. Plumes included in this analysis were intersected 0.3–2.5 h after original emission and had R^2 correlation coefficients greater than or equal to 0.75. Figure 2d shows the geometric mean and range of NO_y/CO_2 emission ratios observed at each industrial complex for each field campaign. Despite the day-to-day variability, the emission ratios show a decreasing trend in NO_x emissions. A linear fit to the ratios, weighted by an imprecision of 30% for each data point, indicates a change and 1-sigma uncer-

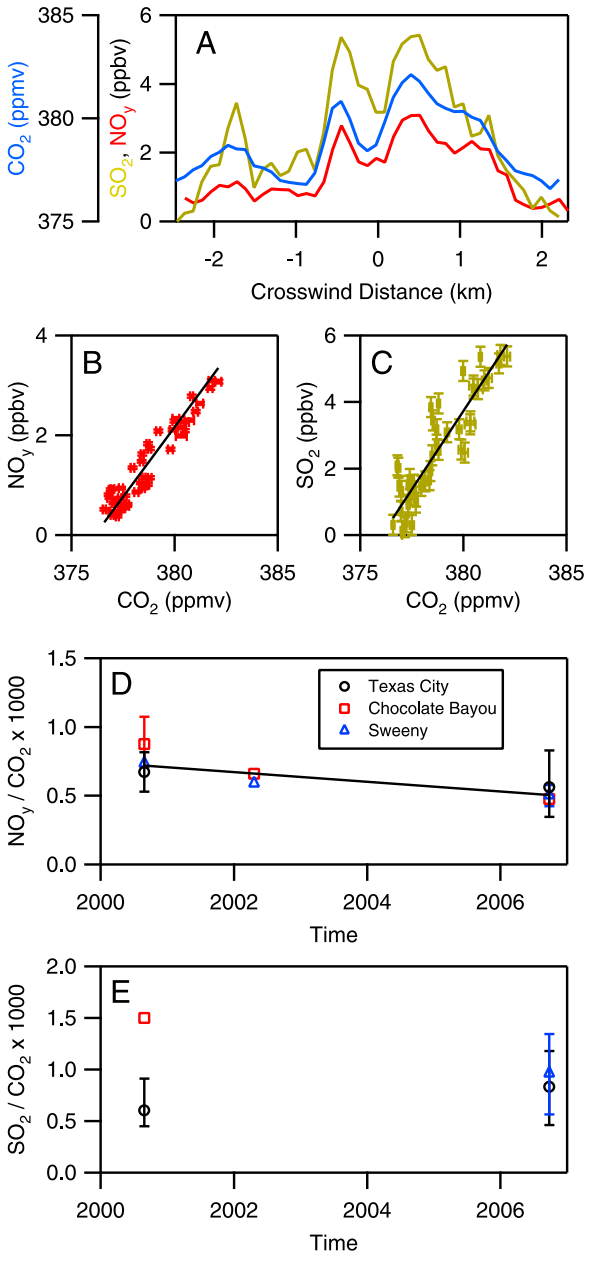

Figure 2. (a) Time series of NO_y, SO_2, and CO_2 measured downwind of the Sweeny industrial complex on 21 September 2006. (b) Correlation plot showing the relationship between NO_y and CO_2 for the Sweeny plume transect. A linear fit to the data, weighted by the imprecision, gives an R^2 correlation coefficient of 0.91. (c) Similar correlation plot showing the relationship between SO_2 and CO_2. A linear fit to the data, weighted by the imprecision, gives an R^2 correlation coefficient of 0.81. (d) Emission ratios were calculated for all industrial plumes intersected by the NOAA WP-3D aircraft during 2000, 2002, and 2006, following the method shown in Figures 2a, 2b, and 2c. Plumes included in this analysis were intersected 0.3–2.5 h after original emission and had an R^2 correlation coefficient greater than or equal to 0.75. The panel shows the geometric mean and annual range of emission ratios observed at each industrial complex. A linear fit to the ratios, weighted by an imprecision of 30% for each data point indicates a decrease in NO_y/CO_2 of 29% ± 20% between August 2000 and September 2006. (e) Similar analysis as in Figure 2d for emission ratios of SO_2/CO_2. A linear fit to the ratios, weighted by an imprecision of 30% for each data point, indicates a statistically insignificant decrease in SO_2/CO_2 of 22% ± 35%.

tainty in NO_y/CO_2 of −29% ± 20% between August 2000 and September 2006. CO_2 emissions scale quantitatively with the mass of fuel consumed, so this result shows that the emissions of NO_x per unit of CO_2 has decreased. Figure 2e indicates no significant trend in SO_2/CO_2 emission ratios.

[21] The error bars in Figures 2d and 2e show the range of values observed during each year and indicate the variability between repeated measurements. Since each industrial complex contains numerous individual processes, which may run discontinuously, it is likely that this variability is real. Recent analysis of aircraft measurements found that NO_x and SO_2 to CO_2 emission ratios for large power plants agree with available CEMS measurements of stack exhaust within ±14% [*Peischl et al.*, 2010]. This measurement uncertainty represents the uncertainty of emission ratios calculated for each individual plume transect.

3.3. Major Contributors to Ozone Formation

[22] Effective air quality regulations require quantification of the relative contribution of NO_x and different VOC species to ozone formation. The importance of an individual hydrocarbon species to ozone formation depends both on its concentration, reactivity, and the reactivity of subsequent reaction products. The relative impacts of different hydrocarbons on urban ozone production can be determined to first order from their OH reactivity, because the initial peroxy radical formation is the rate-limiting step in ozone formation. This comparison is approximate, because it considers only the OH reactivity of the initial VOC species and not the subsequent chemistry of its products. OH reactivity is calculated as the product of the hydrocarbon concentration and its OH reaction rate coefficient at the measured ambient pressure and temperature, according to the expression,

$$R_{OH,\,VOC} = k_{OH+VOC}[VOC]. \quad (1)$$

[23] The actual amount of ozone produced during the oxidation of a particular hydrocarbon species depends on the subsequent reaction products, meteorology, and the concentrations of other hydrocarbons and NO_x [*Carter*, 1994]. However, the relative OH reactivity of different hydrocarbons provides a simple method for comparing their impact on ozone production. In particular, this method allows the instantaneous reactivity of hydrocarbons measured in a complex mixture to be directly compared.

[24] Mixing ratios of an extensive suite of VOC compounds were acquired during summer 2000 at a ground-based site southeast of the Houston Ship Channel [*Jobson et al.*, 2004]. These included CO, C_2–C_{10} alkanes, C_2–C_5 alkenes, ethyne, C_6–C_9 aromatics, and C_2–C_5 aldehydes and ketones. The authors found that reactivity was dominated by C_1–C_3 aldehydes, with ethene and propene occasionally dominating in highly concentrated plumes. During 2006, a similar suite of VOC measurements acquired onboard the NOAA R/V *Ronald H. Brown* in the Gulf of Mexico, Galveston Bay, and the Houston Ship Channel [*Gilman et al.*, 2009] showed that CO and CH_4 dominated OH reactivity in the Gulf of Mexico, while VOCs from anthropogenic sources played the dominant role in Galveston Bay and the Houston Ship Channel. Ethene, propene, and formaldehyde were the largest contributors to OH reactivity, despite the higher mixing ratios of C_2–C_4 alkanes. By examining diurnal profiles, the authors determined that formaldehyde was produced predominantly by secondary chemistry rather than from primary emissions. This contradicts an analysis that correlates formaldehyde with other species and concludes that the formaldehyde budget is dominated by primary sources [*Rappengluck et al.*, 2010].

[25] Aircraft measurements of VOCs provide important information that extends what is available from ground- and ship-based data sets by sampling VOC emissions directly downwind of selected sources. During 2000, 2002, and 2006, whole air samples acquired in the isolated industrial plumes show elevated mixing ratios for many hydrocarbons, including alkanes, alkenes, aromatics, and ethyne. The most abundant VOCs observed in whole air samples acquired in industrial plumes were ethane (C_2H_6), ethene (C_2H_4), propane (C_3H_8), propene (C_3H_6), and isomers of butane (C_4H_{10}) and pentane (C_5H_{12}). In some cases, 1,3-butadiene (C_4H_6) and isomers of butene (C_4H_8) and pentene (C_5H_{10}) were also abundant. OH reactivities for the measured VOCs and NO_2 are presented for the industrial sources in Houston in the following subsections. The OH reaction rate coefficients used here to calculate OH reactivity are taken from several references [*Atkinson*, 1986, 1994, 1997; *DeMore et al.*, 1997; *Atkinson et al.*, 2005; *Sander et al.*, 2006].

3.3.1. Houston Ship Channel

[26] The Houston Ship Channel is the largest complex of industrial sources of NO_x and reactive VOCs in the Houston-Galveston-Brazoria area, so the relative contribution of different VOCs to ozone formation is particularly important for this conglomeration of sources. Figure 3 presents measurements from a representative transect downwind of the Houston Ship Channel on 26 September 2006. Emission sources in the Houston Ship Channel are shown in Figure 3a. Figure 3b shows mixing ratios of NO_x, SO_2, and CO_2 observed during the transect. It is not always possible to attribute specific plumes to individual sources, although some geographical groupings can be made. For example, the large SO_2 source at the west end of the Houston Ship Channel is attributed to industrial sulfuric acid manufacturing.

[27] Figure 3c shows OH reactivity in the Houston Ship Channel plume for the 1 Hz NO_2, CH_2O, and semicontinuous CH_3CHO data. The discrete bars represent the seven second sampling period of the whole air sampler, with formaldehyde and PTR-MS measurements (including acetaldehyde and isoprene) interpolated onto this time base. CO and CH_4 are excluded. Figure 3c shows that anthropogenic VOCs in the Houston Ship Channel are a major contributor to ozone formation. During this transect, total OH reactivity when formaldehyde measurements were available varied between 6.5 and 9.3 s^{-1}, consistent with daytime observations made onboard the R/V *Brown* in the Houston Ship Channel [*Gilman et al.*, 2009]. Although anthropogenic alkane emissions contribute to the OH reactivity, the total is dominated by ethene, propene, formaldehyde, and acetaldehyde. Formaldehyde and acetaldehyde are each formed primarily as secondary products from the oxidation of ethene and propene [*Wert et al.*, 2003]. In contrast, the OH reactivity attributed to biogenic isoprene and other biogenic VOCs is comparatively small in the Houston Ship Channel.

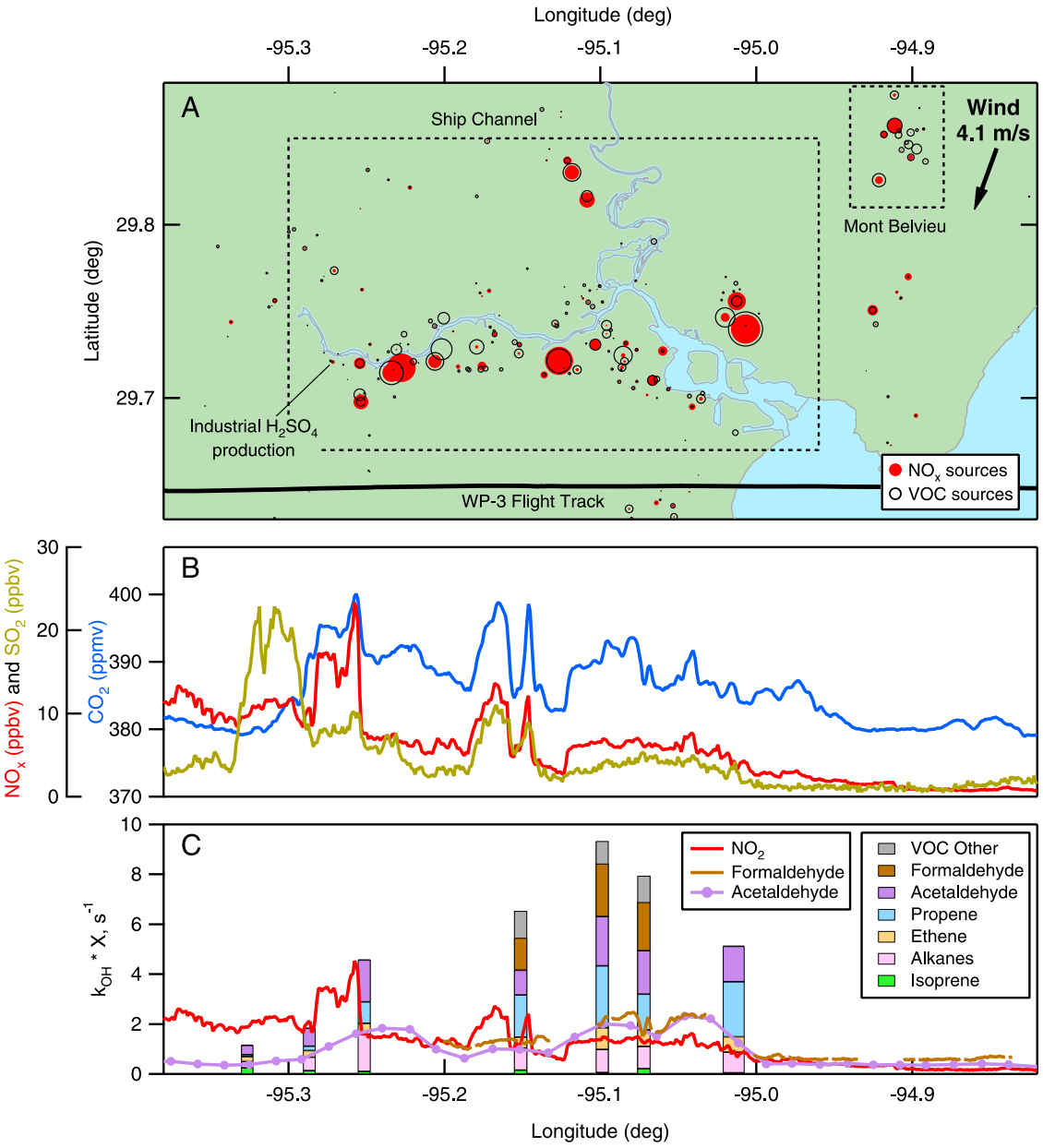

Figure 3. Measurements conducted by the NOAA WP-3D aircraft downwind of the Houston Ship Channel on 26 September 2006. (a) Map of the Houston Ship Channel. TCEQ 2006 PSEI values for NO_x (solid red circles) and VOC (open black circles) are shown. The flight track of the NOAA WP-3D is shown as a black line. Wind direction is from the northeast. (b) Time series of NO_x, SO_2, and CO_2 measured along the flight track. (c) Solid bars showing OH reactivity for isoprene (green), alkanes (pink), ethene (orange), propene (blue), acetaldehyde (purple), formaldehyde (brown), and other measured VOC species (gray). CO and CH_4 are excluded from the reactivity calculation. OH reactivity with NO_2 (red), formaldehyde (brown), and acetaldehyde (purple) are shown as semicontinuous traces.

This is consistent with other measurements in the ship channel that showed the importance of anthropogenic alkene emissions [*Kleinman et al.*, 2002; *Ryerson et al.*, 2003; *Wert et al.*, 2003; *Jobson et al.*, 2004; *Gilman et al.*, 2009].

3.3.2. Other Industrial Sources

[28] High VOC emissions are typical not only for the Houston Ship Channel but also for other industrial facilities in the Houston area. Ozone precursors at the other industrial complexes with fewer individual sources than the Houston Ship Channel can similarly be examined to give insight into the reactivity and relative importance of VOC species. Figure 4 shows representative transects downwind of Texas City, Chocolate Bayou, Freeport, and Sweeny acquired on 19 and 29 September 2006. Each of the industrial complexes shown in Figure 4 has comparable or greater OH reactivity with VOCs than with NO_2. Similar to the Houston Ship

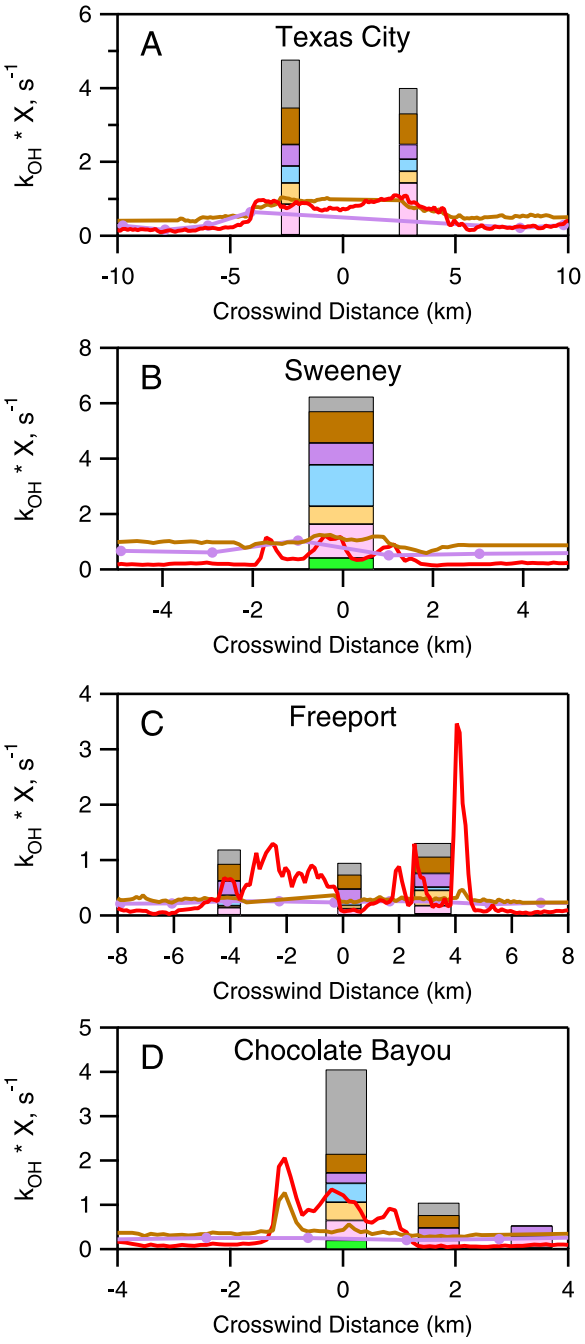

Figure 4. Calculated OH reactivity for NO_2 and VOCs measured by a whole air sampler for representative plume transects of (a) Texas City, (b) Sweeny, (c) Freeport, and (d) Chocolate Bayou, using the same color scheme as in Figure 3c. The Texas City and Sweeny plumes were measured on 19 September 2006. The Freeport and Chocolate Bayou plumes were measured on 29 September 2006. The *x* axis indicates the cross-plume distance, with 0 km at the center of the plume. The unspeciated OH reactivity for Chocolate Bayou is dominated by 1,3-butadiene and 1-butene.

Channel, ethene, propene, formaldehyde, and acetaldehyde are major contributors to the OH reactivity. For transects downwind of Texas City, Sweeny, and Freeport, these VOCs account for more than half of the OH reactivity. At Chocolate Bayou, the reactivity includes an additional contribution from 1-butene and 1,3-butadiene. These highly reactive compounds may be emitted by other facilities as well but are rapidly removed in the atmosphere by oxidation. Both Sweeny and Chocolate Bayou indicate a larger OH reactivity due to isoprene than is observed in the Houston Ship Channel. This is expected from biogenic emission inventories for the region [*Wiedinmyer et al.*, 2001; *Warneke et al.*, 2010]. At Freeport, the fraction of OH reactivity attributed to VOCs is smaller than at the other complexes.

[29] Elevated ethene, propene, formaldehyde, and acetaldehyde concentrations are consistently observed downwind of industrial sources in the aircraft measurements. Previous analysis of ethene measurements concluded that emissions from mobile sources were small downwind of the Houston urban core [*de Gouw et al.*, 2009]. Similarly, we observe here that ethene, propene, formaldehyde, and acetaldehyde are predominantly associated with industrial point sources and not mobile sources.

3.4. Temporal Trends in Ethene and Propene Emissions for Industrial Sources

[30] According to the calculations of OH reactivity presented in Figures 3 and 4, ethene and propene are two of the most significant VOC precursors to ozone formation from industrial sources in Houston. The aircraft data acquired in 2000, 2002, and 2006 can be used to determine emission trends and variability for ethene and propene. Previous studies in 2000 showed substantial discrepancies between emission inventories and measurements for these highly reactive VOCs [*Ryerson et al.*, 2003; *Wert et al.*, 2003]. We can compare the ethene and propene emissions measured in 2006 to the TCEQ PSEI to quantify the agreement and examine changes.

3.4.1. C_2H_4/NO_x and C_3H_6/NO_x Ratios

[31] Emission ratios are the best choice for comparing the aircraft measurements of ethene and propene emissions to the TCEQ Point Source Emissions Inventory and examining temporal trends in their emissions. For the sparse samples acquired by the whole air sampler, it is not possible to calculate absolute fluxes. Continuous ethene measurements were acquired by the LPAS instrument, and these data were used to determine emission fluxes for ethene from the Mont Belvieu chemical complex [*de Gouw et al.*, 2009]. However, ethene concentrations in some plume transects analyzed here were at or near the detection limit of the LPAS.

[32] When conserved species are coemitted from a single large source, their enhancement ratio should remain constant as the plume is transported downwind and diluted. However, their ratio will change if chemical or physical processes preferentially remove one of the species. The location of NO_x and VOC emissions within a facility do not have to coincide, as long as the plume is well mixed at the time of downwind sampling. For the Texas City, Chocolate Bayou, Freeport, and Sweeny industrial complexes, we use aircraft measurements acquired during plume transects in 2000, 2002, and 2006 to calculate emission ratios of C_2H_4/NO_x

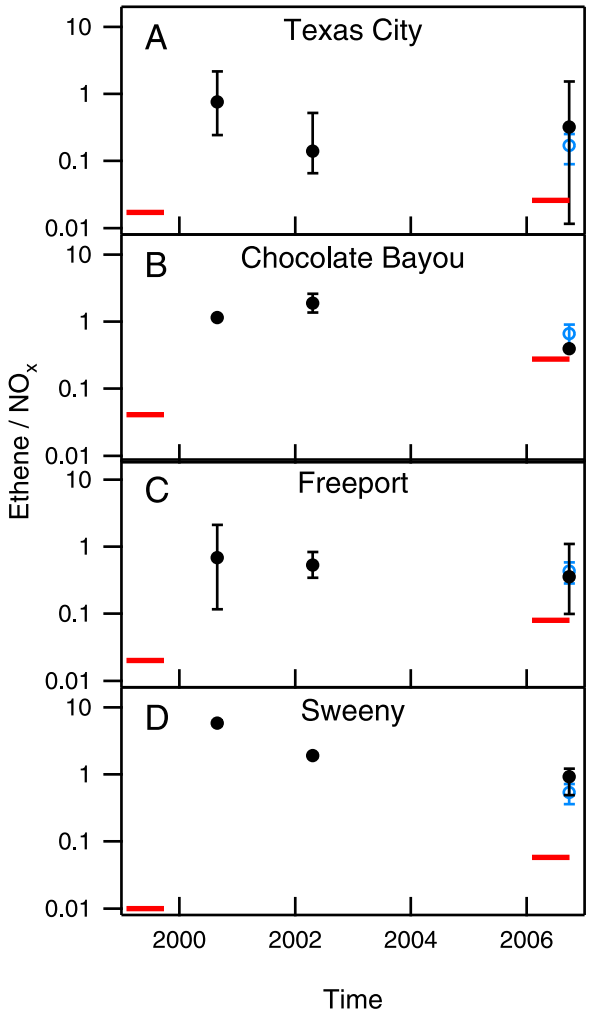

Figure 5. Measurements of C_2H_4/NO_x ratio by the NOAA WP-3D in 2000, 2002, and 2006 (solid black circles) with measured range indicated for (a) Texas City (26 samples; 11 dates), (b) Chocolate Bayou (6 samples; 3 dates), (c) Freeport (22 samples; 5 dates), and (d) Sweeny (11 samples; 6 dates). C_2H_4/NO_x measurements by solar occultation flux technique [*Mellqvist et al.*, 2010] in 2006 are shown as open blue circles. Ratio calculated from TCEQ PSEI is shown as solid red bar.

and C_3H_6/NO_x. The daytime plumes examined in this work were intersected 0.2–2.7 h (2–61 km) downwind of the industrial complexes, as calculated from the average wind speed at the time of plume intersection and the distance from the source. Reaction with OH is the primary loss mechanism for C_2H_4, C_3H_6, and NO_2. The respective OH reaction rates of these molecules at standard temperature and pressure (298 K; 1013 mb) are 9.1×10^{-12}, 30.2×10^{-12}, and 10.6×10^{-12} cm^3 $molecule^{-1}$ s^{-1} [*Atkinson et al.*, 2005; *Sander et al.*, 2006]. This indicates that the C_2H_4/NO_x enhancement ratio will be approximately conserved downwind. In contrast, the measured C_3H_6/NO_x ratio can only be considered a lower limit of the original C_3H_6/NO_x emission ratio because of the greater OH reactivity of C_3H_6.

[33] Figure 5 shows the observed ratio of C_2H_4/NO_x for plume transects acquired during 2000, 2002, and 2006 downwind of the four industrial complexes. The solid black circles indicate the geometric mean emission ratio and range. The four panels are plotted on a log scale to better compare with the C_2H_4/NO_x ratio calculated from the TCEQ Point Source Emissions Inventory. Table 3 gives the number of samples, mean, median, range, and emission inventory values for the 2006 data at each of the four industrial complexes. The measured C_2H_4/NO_x ratios exceed the emission inventory values by factors of 1.4–20. Independent flux measurements acquired in 2006 by solar occultation flux and DOAS [*Mellqvist et al.*, 2010; *Rivera et al.*, 2010] are shown in Figure 5, and these agree well with the aircraft determinations. The consistent disagreement between the measurements and emissions inventory over multiple sampling dates and multiple years makes it unlikely that the high ethene emissions are due to upsets or nonroutine emission events. The discrepancies between the emissions inventory and the measurements are consistently large.

[34] Identifying temporal trends in the C_2H_4/NO_x ratio from Figure 5 is difficult. For the NO_x/CO_2 and SO_2/CO_2 ratios presented in Figure 2, the uncertainty in the individual ratio determinations is comparable to the variability between repeated measurements. For the C_2H_4/NO_x and C_3H_6/NO_x ratios, the variability is higher than the measurement uncertainty. The day-to-day and within-plume variability is large (approximately −50% to +100%), as indicated by the range bars. This is consistent with previous studies that reported variability in ethene emissions [*Murphy and Allen*, 2005; *de Gouw et al.*, 2009; *Mellqvist et al.*, 2010]. It appears that decreases in ethene emissions relative to NO_x may have occurred at the Sweeny industrial complex. For the other industrial complexes, any interannual trend is hidden by variability within the plume and between different days.

[35] Figure 6 shows the observed ratio of C_3H_6/NO_x for the same plume transects as displayed in Figure 5. As for ethene, the solid black circles indicate the average emission ratio and range. As described above, the measured C_3H_6/NO_x ratio represents a lower limit of the actual emission ratio due to the higher reactivity of C_3H_6 relative to NO_2. Like the C_2H_4/NO_x ratios in Figure 5, the measured C_3H_6/NO_x ratios in Figure 6 exceed the emission inventory values by factors of 1–24. This indicates that the actual discrepancy between measurements and the TCEQ Point Source Emis-

Table 3. VOC/NO_x Ratios Measured for Plume Transects During 2006 Compared to TCEQ Point Source Emissions Inventory Values[a]

	C_2H_4/NO_x				
	n	Mean	Median	Range	E.I.
Texas City	17	0.32	0.39	0.01–1.5	0.03
Chocolate Bayou	3	0.40	0.38	0.38–0.42	0.28
Freeport	4	0.36	0.61	0.04–1.1	0.08
Sweeny	7	0.93	1.1	0.49–1.2	0.06
	C_3H_6/NO_x				
	n	Mean	Median	Range	E.I.
Texas City	18	0.11	0.16	0.002–0.75	0.02
Chocolate Bayou	3	0.12	0.13	0.08–0.15	0.13
Freeport	4	0.05	0.07	0.02–0.13	0.01
Sweeny	7	0.68	0.65	0.48–1.1	0.03

[a]Geometric mean is given.

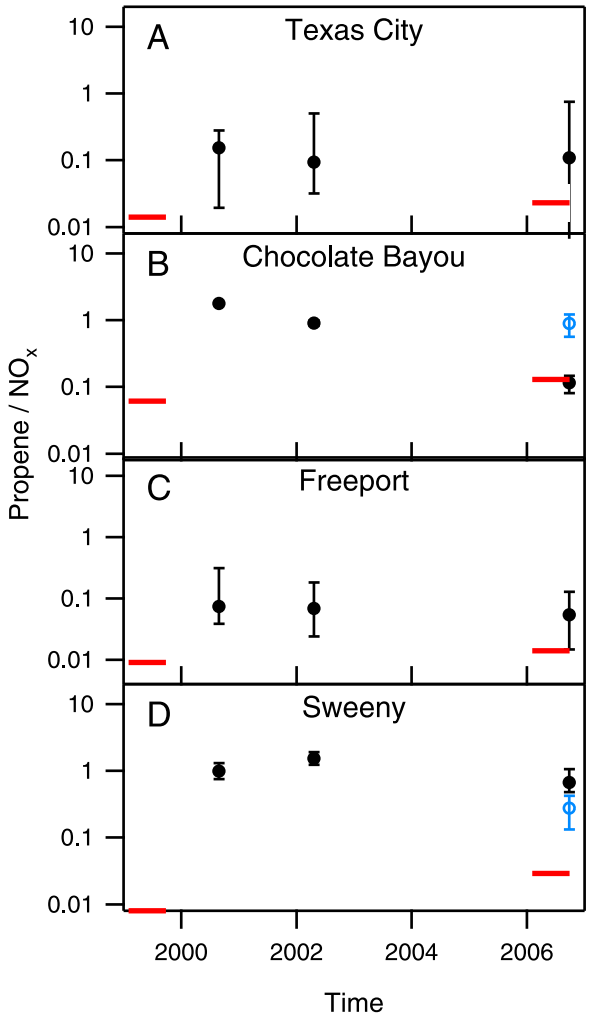

Figure 6. Measurements of C_3H_6/NO_x ratio by the NOAA WP-3D in 2000, 2002, and 2006 shown similarly as in Figure 5.

sions Inventory for C_3H_6 is even greater than it is for C_2H_4. Independent flux measurements acquired in 2006 by solar occultation flux and DOAS [*Mellqvist et al.*, 2010; *Rivera et al.*, 2010] are shown as open blue circles with their calculated error bars. Again, the discrepancy between the emissions inventory and the measurements appears to be real. The day-to-day and within-plume variabilities are large, as indicated by the range bars, obscuring temporal trends in the C_3H_6/NO_x ratio. It appears that C_3H_6 emission reductions relative to NO_x may have occurred at the Chocolate Bayou industrial complex. For the other industrial complexes, any interannual trend is hidden by variability within the plume and between different days.

[36] The large discrepancies shown in Figures 5 and 6 between C_2H_4/NO_x and C_3H_6/NO_x ratios reported in the TCEQ PSEI and measured by the WP-3D could be due to inaccuracy in the alkene emissions, NO_x emissions, or both. Previous work has shown that NO_x is better represented than VOCs in available point source emission inventories [*Ryerson et al.*, 2003]. NO_x emissions in the TCEQ PSEI are derived from CEMS data for many of the large NO_x sources at each industrial complex. As discussed in section 3.2, the CEMS emission ratios have been verified within ±14% [*Peischl et al.*, 2010] and the EPA requires the absolute accuracy to be within ±10%. Additionally, previous calculations of NO_y mass flux for industrial sources during the TexAQS 2000 campaign showed agreement with emission inventories within ±50% [*Ryerson et al.*, 2003]. There is no evidence that NO_x inventory values are inaccurate by more than this factor in Houston. Thus, the large inventory discrepancies in C_2H_4/NO_x and C_3H_6/NO_x ratios shown in Figures 5 and 6 are unlikely due to errors in inventory NO_x values. These discrepancies are more likely attributed to C_2H_4 and C_3H_6 emissions that are consistently much higher than represented in the TCEQ PSEI. C_2H_4 and C_3H_6 emissions from industrial sources that are much higher than values in the inventory have been observed during every flight in Houston during 2000, 2002, and 2006. These higher emissions were not reported as flares or upset events, but instead represent typical operating conditions in the Houston urban area.

[37] Examination of the temporal trends for C_2H_4/NO_x and C_3H_6/NO_x ratios further requires consideration of how both VOC and NO_x concentrations change through time. Trends in NO_x emissions, as observed in NO_x/CO_2 ratios for the industrial complexes, were discussed in detail in section 3.2. The TCEQ PSEI indicates NO_x reductions of 40%–84% (see Table 2), and the WP-3D measurements show reductions of 29% ± 20% (see Figure 2d). We estimate the total change in emissions of C_2H_4 and C_3H_6 for the industrial complexes over the 2000–2006 period to be −30% ± 30%.

3.4.2. Ambient C_2H_4 and C_3H_6 Concentrations

[38] The previous section presented emission ratios that can be linked to known industrial sources. It is also possible to examine trends in ambient C_2H_4 and C_3H_6 concentrations observed during 2000 and 2006 onboard the NOAA aircraft. Figure 7a shows a geographical box that includes the Houston Ship Channel, Mont Belvieu industrial complex, and the Houston urban core. During 2000 and 2006, 117 and 273 whole air samples, respectively, were acquired within this sampling area at an aircraft altitude of 200–1000 m. Figures 7b and 7c show the cumulative probability distributions for ethene and propene mixing ratios measured during each of the two years. The median observed value changed by −52% and −48% for ethene and propene, respectively. Although the mean concentrations may be biased by high values, the mean has a well-defined uncertainty that is useful for evaluating whether the trend is significant. The mean concentration changes for ethene and propene were −52% ± 8% and −52% ± 21%, respectively. Surface measurements acquired during 2000 and 2006 have also indicated a decrease in ambient concentrations of C_2H_4 and C_3H_6 [*Gilman et al.*, 2009]. Reductions in measured VOC concentrations may be due either to reductions in emissions or to differences in meteorology that result in different dilution or oxidation of the emissions. Fully quantifying the potential differences in boundary layer heights, solar radiation, and mixing during the two years is difficult. However, all emissions are subject to the same meteorology. Ethyne, shown in Figure 7d, is emitted in vehicle exhaust and is typically used as an urban tracer. The cumulative probability plot for ethyne shows a more modest change in the median value between 2000 and 2006 of −10%. The trend in the mean concentration of ethyne was −37% ± 10%.

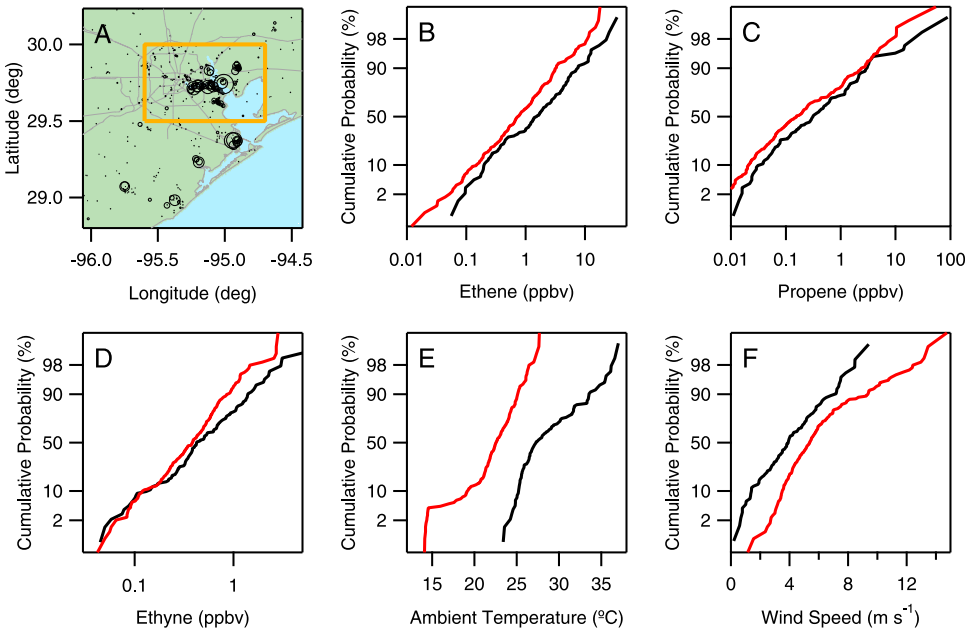

Figure 7. (a) Map of Houston, Texas, showing geographical box (bordered by 29.500°N 95.600°W and 30.000°N 94.700°W). Cumulative probabilities were calculated for VOCs acquired by the whole air sampler and coincident measurements between 200 and 1000 m altitude within this box shown for the years 2000 (black) and 2006 (red). Median concentrations in 2000 and 2006 respectively for each plot: (b) ethene, 1.53 and 0.73 ppbv; (c) propene, 0.31 and 0.16 ppbv; (d) ethyne, 0.42 and 0.38 ppbv; (e) wind speed, 3.9 and 5.4 m s^{-1}; (f) ambient temperature, 27.3°C and 22.5°C.

Analysis of CO, another urban tracer, shows a change in the median value of −18.0% during this same time period, with a trend in the mean concentration of −17% ± 3%. Figures 7e and 7f show the calculated cumulative probability for ambient temperature and wind speed observed during the 2 years. Average wind speeds were higher in 2006 than in 2000, which would lead to a greater dilution of ethene emissions and lower mixing ratios in 2006. Conversely, average temperatures were lower in 2006 than in 2000, consistent with observations of shallower boundary layers and less vigorous vertical mixing, which would lead to higher mixing ratios in 2006. A similar cumulative analysis of formaldehyde, the main photooxidation product of ethene, for 2000 and 2006 in the same geographical area shows that its median concentration decreased by more than 40%. The changes in the ambient concentrations of all of these species are consistent with the conclusion that the decreases in C_2H_4 concentration are due to decreases in emissions, rather than to differences in meteorological conditions between the two data sets.

3.5. Secondary Photochemical Products Formed Downwind

[39] The large suite of measurements onboard the NOAA WP-3D aircraft makes it possible to examine chemical processing downwind of the industrial complexes. Oxidation of each of the alkene species results in different photochemical products. Initially, alkenes react with OH, O_3, or NO_3 to form ketones and aldehydes. The carbon-carbon double bond is broken, forming two carbonyl groups. The aldehydes proceed to react with OH or photolyze. In particular, terminal alkenes react with OH to form formaldehyde, which may subsequently react with OH to yield a hydroperoxy radical and CO, or photolyze through one of two pathways. 2-Alkenes react with OH to form acetaldehyde, which may then react with OH in the presence of NO_2 to form peroxyacetyl nitrate (PAN). Using the NOAA WP-3D measurements, we can identify the ketone, aldehyde, and PAN reaction products downwind.

[40] A series of three WP-3D transects acquired downwind of the Texas City industrial complex on 19 September 2006 is shown in Figure 8a. The portion of each flight track crossing the plume is shown in black, with measured NO_x plotted in red to indicate the plume location. The plume was intersected at distances of 19.6, 41.3, and 56.0 km downwind, corresponding to plume ages of 0.6, 1.5, and 2.3 h. As discussed previously and shown in Figure 4a, the Texas City industrial complex emits high concentrations of reactive VOCs and NO_x. Figures 8b and 8c show the mixing ratios of primary emissions (ethene, propene, and NO_x) and secondary photochemical products (formaldehyde, acetaldehyde, PAN, and O_3) during the first and third transects. The initially high ethene concentrations observed within the first transect are greatly decreased by the third transect, as seen in the continuous LPAS ethene data and single WAS sample, demonstrating the high reactivity of ethene. Similarly, while NO_x accounts for more than half of the NO_y observed in the first transect, it has been largely oxidized by the third transect.

[41] The loss rates of the primary emissions and production rates of the secondary photochemical products can be calculated by assuming that NO_y is a conserved plume tracer over the transport time of these three transects. Figure 8d shows ln(VOC/NO_y) ratios for ethene and propene as a function of downwind transport time with linear fits weighted by the measurement imprecision. The corresponding expo-

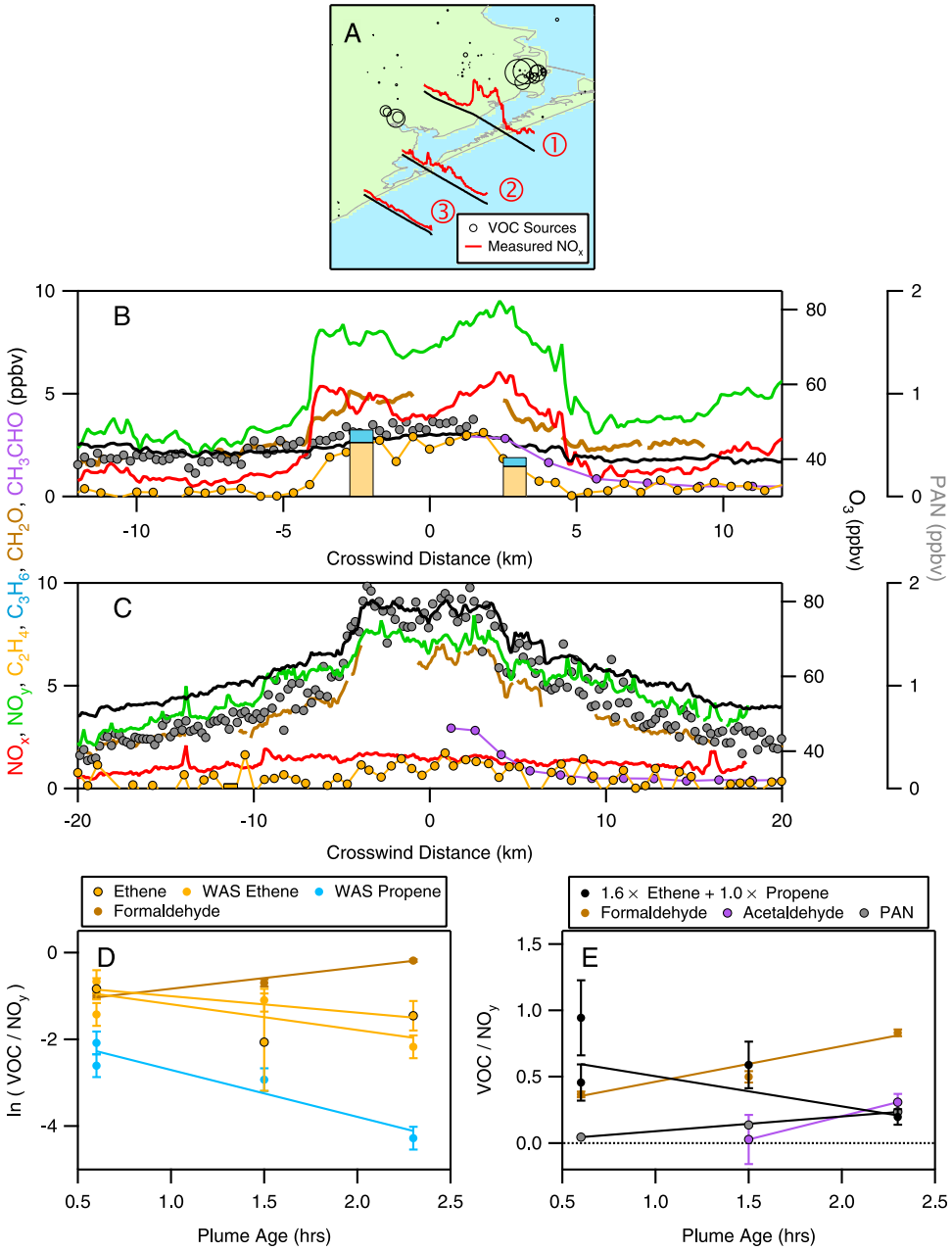

Figure 8. (a) Map of three transects measured downwind of the Texas City complex on 19 September 2006. Measured NO_x is plotted on the map, indicating the plume location. (b and c) Primary emissions and secondary photochemical products measured during the first and third downwind transects. The *x* axis indicates the cross-plume distance, with 0 km at the center of the plume. Primary emissions include ethene (orange bar) and propene (blue bar) measured by the whole air sampler, ethene measured by LPAS (solid orange circles) and NO_x (red line). Secondary photochemical products include formaldehyde (brown line), acetaldehyde (solid purple circles), NO_y (green line), PAN (solid gray circles), and O_3 (black line). (d) Natural log of the ratio of VOC species to NO_y, as a function of transport time downwind. NO_y is used here as an approximately conserved plume tracer. Slopes for ethene measured by the LPAS and whole air sampler are -0.4 ± 0.2 and -0.6 ± 0.2 h^{-1}, respectively. The slope for propene is -1.1 ± 0.2. (e) Ratios of VOC photochemical products to NO_y. The slopes for formaldehyde, acetaldehyde, and PAN are 0.27 ± 0.02, 0.35 ± 0.24, and 0.112 ± 0.004 ppbv ppbv^{-1} h^{-1}. The slope of 1.6 × ethene + 1.0 × propene is -0.22 ± 0.08 ppbv ppbv^{-1} h^{-1}.

nential decay rate of ethene for the LPAS instrument and whole air sampler are -0.4 ± 0.2 and -0.6 ± 0.2 h^{-1}, respectively. The observed propene loss is -1.1 ± 0.2 h^{-1}. Figure 8e shows the production rates of formaldehyde, acetaldehyde and PAN as 0.27 ± 0.02, 0.35 ± 0.24, and 0.112 ± 0.004 ppbv ppbv^{-1} h^{-1}. The sum of $1.6 \times C_2H_4/NO_x + 1.0 \times C_3H_6/NO_x$ represents a formaldehyde yield of 1.6 for ethene [*Niki et al.*, 1981] and 1.0 for propene [*Niki et al.*, 1978]. This sum has a fitted slope of -0.22 ± 0.08 ppbv ppbv^{-1} h^{-1}, indicating that the loss of these two alkenes accounts for more than 80% of the observed formaldehyde production, neglecting photochemical losses for formaldehyde. The propene losses are insufficient to account for the production of acetaldehyde and PAN, indicating that other 2-alkenes may by important in the carbon budget for these two secondary products.

4. Conclusions

[42] Observed reductions of 29% ± 20% in NO_x emissions at the industrial complexes between August 2000 and September 2006 are consistent with observations of reduced NO_x emissions at larger power plants throughout the southeastern United States that have implemented emission abatement controls. Previous analysis of industrial emissions measured during the TexAQS 2000 field campaign showed that the principal VOC precursors leading to the rapid ozone formation characteristic of the Houston-Galveston-Brazoria area were petrochemical emissions of ethene and propene. Our examination of temporal trends in C_2H_4/NO_x and C_3H_6/NO_x ratios from isolated petrochemical sources between 2000 and 2006 leads to the conclusion that emissions of these alkenes have decreased by 30% ± 30%. Additionally, we observe that median ambient concentrations of ethene and propene within the Houston urban area have changed by −52% and −48%, respectively, over this same time period. One principal result from the 2000 field study was the identification of large underestimates of reactive light alkenes in VOC emission inventories for petrochemical sources [*Kleinman et al.*, 2002; *Karl et al.*, 2003; *Ryerson et al.*, 2003; *Wert et al.*, 2003; *Jobson et al.*, 2004]. The analysis presented here for 2000, 2002, and 2006 measurements in the Houston-Galveston-Brazoria area indicates that emission inventory inaccuracies persist. Measured ratios of C_2H_4/NO_x and C_3H_6/NO_x exceed emission inventory values by factors of 1.4–20 and 1–24, respectively. *De Gouw et al.* [2009] reported ethene emissions of 520 ± 140 kg h^{-1} from the Mont Belvieu industrial complex. Comparing those measurements to the updated 2006 emission inventory shown in Table 2 gives a factor of 6 discrepancy, which is similar to the results reported here for other industrial complexes. Because of the inaccurate accounting of ethene, propene, and other reactive VOC emissions in the 2006 TCEQ PSEI, chemical transport models will continue to have difficulty in accurately predicting ozone levels in the greater Houston area. Although the current analysis has focused on the isolated petrochemical industrial areas, including Texas City, Chocolate Bayou, Sweeny, and Freeport, the largest source in this area remains the Houston Ship Channel. The high concentration of colocated NO_x and VOC sources in the Houston Ship Channel make it difficult to analyze, but it is certainly a major contributor to ozone formation.

[43] **Acknowledgments.** We thank the management, staff, and flight crew from the NOAA Aircraft Operations Center for their support during the field mission. We thank Bryan Lambeth and TCEQ for the La Porte wind profiler data. We thank John Jolly for TCEQ emissions inventory data. We thank Johan Mellqvist, Claudia Rivera, and Jerker Samuelsson for sharing their solar occultation flux and DOAS measurements. We thank Dr. Sacco te Lintel Hekkert from Sensor Sense for LPAS measurements. R.A.W. thanks Dr. Chuck Brock for helpful discussions. We acknowledge financial support for the field measurements from the NOAA Air Quality and NOAA Climate Research and Modeling programs. We acknowledge financial support for the analysis from Texas Commission on Environmental Quality contract 582-8-86246-FY09. R.A.W. acknowledges a National Research Council Postdoctoral Fellowship.

References

Atkinson, R. (1986), Kinetics and mechanisms of the gas-phase reactions of the hydroxyl radical with organic-compounds under atmospheric conditions, *Chem. Rev.*, *86*(1), 69–201.

Atkinson, R. (1994), Gas-phase tropospheric chemistry of organic-compounds, *J. Phys. Chem. Ref. Data*.

Atkinson, R. (1997), Gas-phase tropospheric chemistry of volatile organic compounds: 1. Alkanes and alkenes, *J. Phys. Chem. Ref. Data*, *26*(2), 215–290.

Atkinson, R., D. L. Baulch, R. A. Cox, J. N. Crowley, J. R. F. Hampson, R. G. Hynes, M. E. Jenkin, J. A. Kerr, M. J. Rossi, and J. Troe (2005), Summary of evaluated kinetic and photochemical data for atmospheric chemistry, IUPAC Subcomm. on Gas Kinet. Data Eval. for Atmos. Chem., Research Triangle Park, NC.

Carter, W. P. L. (1994), Development of ozone reactivity scales for volatile organic-compounds, *J. Air Waste Manage. Assoc.*, *44*(7), 881–899.

Crutzen, P. J. (1979), Role of NO and NO_2 in the Chemistry of the Troposphere and Stratosphere, *Annu. Rev. Earth Planet. Sci.*, *7*, 443–472.

Daum, P. H., L. Kleinman, D. G. Imre, L. J. Nunnermacker, Y. N. Lee, S. R. Springston, L. Newman, and J. Weinstein-Lloyd (2000), Analysis of the processing of Nashville urban emissions on July 3 and July 18, 1995, *J. Geophys. Res.*, *105*(D7), 9155–9164, doi:10.1029/1999JD900997.

Daum, P. H., L. I. Kleinman, S. R. Springston, L. J. Nunnermacker, Y. N. Lee, J. Weinstein-Lloyd, J. Zheng, and C. M. Berkowitz (2003), A comparative study of O_3 formation in the Houston urban and industrial plumes during the 2000 Texas Air Quality Study, *J. Geophys. Res.*, *108*(D23), 4715, doi:10.1029/2003JD003552.

de Gouw, J., and C. Warneke (2007), Measurements of volatile organic compounds in the Earth's atmosphere using proton-transfer-reaction mass spectrometry, *Mass Spectrom. Rev.*, *26*(2), 223–257.

de Gouw, J. A., P. D. Goldan, C. Warneke, W. C. Kuster, J. M. Roberts, M. Marchewka, S. B. Bertman, A. A. P. Pszenny, and W. C. Keene (2003), Validation of proton transfer reaction-mass spectrometry (PTR-MS) measurements of gas-phase organic compounds in the atmosphere during the New England Air Quality Study (NEAQS) in 2002, *J. Geophys. Res.*, *108*(D21), 4682, doi:10.1029/2004JD003863.

de Gouw, J. A., et al. (2009), Airborne measurements of ethene from industrial sources using laser photo-acoustic spectroscopy, *Environ. Sci. Technol.*, *43*(7), 2437–2442.

DeMore, W. B., S. P. Sander, D. M. Golden, R. F. Hampson, M. J. Kurylo, C. J. Howard, A. R. Ravishankara, C. E. Kolb, and M. J. Molina (1997), Chemical kinetics and photochemical data for use in stratospheric modeling, NASA Jet Propulsion Laboratory, Pasadena, Calif.

Gillani, N. V., J. F. Meagher, R. J. Valente, R. E. Imhoff, R. L. Tanner, and M. Luria (1998), Relative production of ozone and nitrates in urban and rural power plant plumes: 1. Composite results based on data from 10 field measurement days, *J. Geophys. Res.*, *103*(D17), 22,593–22,615.

Gilman, J. B., et al. (2009), Measurements of volatile organic compounds during the 2006 TexAQS/GoMACCS campaign: Industrial influences, regional characteristics, and diurnal dependencies of the OH reactivity, *J. Geophys. Res.*, *114*, D00F06, doi:10.1029/2008JD011525, [printed 115(D7), 2010].

Haagen-Smit, A. J. (1952), Chemistry and physiology of Los Angeles smog, *Ind. Eng. Chem.*, *44*(6), 1342–1346.

Holloway, J. S., R. O. Jakoubek, D. D. Parrish, C. Gerbig, A. Volz-Thomas, S. Schmitgen, A. Fried, B. Wert, B. Henry, and J. R. Drummond (2000), Airborne intercomparison of vacuum ultraviolet fluorescence and tunable diode laser absorption measurements of tropospheric carbon monoxide, *J. Geophys. Res.*, *105*(D19), 24,251–24,261, doi:10.1029/2000JD900237.

Jobson, B. T., C. M. Berkowitz, W. C. Kuster, P. D. Goldan, E. J. Williams, F. C. Fesenfeld, E. C. Apel, T. Karl, W. A. Lonneman, and D. Riemer (2004), Hydrocarbon source signatures in Houston, Texas: Influence of the petrochemical industry, *J. Geophys. Res.*, *109*, D24305, doi:10.1029/2004JD004887.

Karl, T., T. Jobson, W. C. Kuster, E. Williams, J. Stutz, R. Shetter, S. R. Hall, P. Goldan, F. Fehsenfeld, and W. Lindinger (2003), Use of proton-transfer-reaction mass spectrometry to characterize volatile organic compound sources at the La Porte super site during the Texas Air Quality Study 2000, *J. Geophys. Res.*, *108*(D16), 4508, doi:10.1029/2002JD003333.

Kim, S.-W., A. Heckel, S. A. McKeen, G. J. Frost, E. Y. Hsie, M. K. Trainer, A. Richter, J. P. Burrows, S. E. Peckham, and G. A. Grell (2006), Satellite-observed US power plant NO_x emission reductions and their impact on air quality, *Geophys. Res. Lett.*, *33*, L22812, doi:10.1029/2006GL027749.

Kleinman, L. I., P. H. Daum, D. Imre, Y. N. Lee, L. J. Nunnermacker, S. R. Springston, J. Weinstein-Lloyd, and J. Rudolph (2002), Ozone production rate and hydrocarbon reactivity in 5 urban areas: A cause of high ozone concentration in Houston, *Geophys. Res. Lett.*, *29*(10), 1467, doi:10.1029/2001GL014569.

Mellqvist, J., J. Samuelsson, J. Johansson, C. Rivera, B. Lefer, S. Alvarez, and J. Jolly (2010), Measurements of industrial emissions of alkenes in Texas using the Solar Occultation Flux method, *J. Geophys. Res.*, *115*, D00F17, doi:10.1029/2008JD011682.

Murphy, C. F., and D. T. Allen (2005), Hydrocarbon emissions from industrial release events in the Houston-Galveston area and their impact on ozone formation, *Atmos. Environ.*, *39*(21), 3785–3798.

Nielsen-Gammon, J. W., C. L. Powell, M. J. Mahoney, W. M. Angevine, C. Senff, A. White, C. Berkowitz, C. Doran, and K. Knupp (2008), Multisensor estimation of mixing heights over a coastal city, *J. Appl. Meteorol.*, *47*(1), 27–43.

Niki, H., P. D. Maker, C. M. Savage, and L. P. Breitenbach (1978), Mechanism for hydroxyl radical initiated oxidation of olefin nitric oxide mixtures in parts per million concentrations, *J. Phys. Chem.*, *82*(2), 135–137.

Niki, H., P. D. Maker, C. M. Savage, and L. P. Breitenbach (1981), An FTIR study of mechanisms for the HO radical initiated oxidation of C_2H_4 in the presence of NO – detection of glycolaldehyde, *Chem. Phys. Lett.*, *80*(3), 499–503.

Parrish, D. D., et al. (2009), Overview of the Second Texas Air Quality Study (TexAQS II) and the Gulf of Mexico Atmospheric Composition and Climate Study (GoMACCS), *J. Geophys. Res.*, *114*, D00F13, doi:10.1029/2009JD011842, [printed 115(D7), 2010].

Peischl, J., et al. (2010), A top-down analysis of emissions from selected Texas power plants during TexAQS 2000 and 2006, *J. Geophys. Res.*, doi:10.1029/2009JD013527, in press.

Rappengluck, B., P. K. Dasgupta, M. Leuchner, Q. Li, and W. Luke (2010), Formaldehyde and its relation to CO, PAN, and SO_2 in the Houston-Galveston airshed, *Atmos. Chem. Phys.*, *10*(5), 2413–2424.

Rivera, C., J. Mellqvist, J. Samuelsson, B. Lefer, S. Alvarez, and M. R. Patel (2010), Quantification of NO_2 and SO_2 emissions from the Houston Ship Channel and Texas City industrial areas during the 2006 Texas Air Quality Study, *J. Geophys. Res.*, *115*, D08301, doi:10.1029/2009JD012675.

Ryerson, T. B., et al. (1998), Emissions lifetimes and ozone formation in power plant plumes, *J. Geophys. Res.*, *103*(D17), 22,569–22,583, doi:10.1029/98JD01620.

Ryerson, T. B., L. G. Huey, K. Knapp, J. A. Neuman, D. D. Parrish, D. T. Sueper, and F. C. Fehsenfeld (1999), Design and initial characterization of an inlet for gas-phase NO_y measurements from aircraft, *J. Geophys. Res.*, *104*(D5), 5483–5492, doi:10.1029/1998JD100087.

Ryerson, T. B., E. J. Williams, and F. C. Fehsenfeld (2000), An efficient photolysis system for fast-response NO_2 measurements, *J. Geophys. Res.*, *105*(D21), 26,447–26,461, doi:10.1029/2000JD900389.

Ryerson, T. B., et al. (2001), Observations of ozone formation in power plant plumes and implications for ozone control strategies, *Science*, *292*(5517), 719–723.

Ryerson, T. B., et al. (2003), Effect of petrochemical industrial emissions of reactive alkenes and NO_x on tropospheric ozone formation in Houston, Texas, *J. Geophys. Res.*, *108*(D8), 4249, doi:10.1029/2002JD003070.

Sander, S. P., et al. (2006), Chemical Kinetics and Photochemical Data for Use in Atmospheric Studies, NASA Jet Propulsion Laboratory, Pasadena, Calif.

Schauffler, S. M., E. L. Atlas, D. R. Blake, F. Flocke, R. A. Lueb, J. M. Lee-Taylor, V. Stroud, and W. Travnicek (1999), Distributions of brominated organic compounds in the troposphere and lower stratosphere, *J. Geophys. Res.*, *104*(D17), 21,513–21,535, doi:10.1029/1999JD900197.

Schauffler, S. M., E. L. Atlas, S. G. Donnelly, A. Andrews, S. A. Montzka, J. W. Elkins, D. F. Hurst, P. A. Romashkin, G. S. Dutton, and V. Stroud (2003), Chlorine budget and partitioning during the Stratospheric Aerosol and Gas Experiment (SAGE) III Ozone Loss and Validation Experiment (SOLVE), *J. Geophys. Res.*, *108*(D5), 4173, doi:10.1029/2001JD002040.

Slusher, D. L., L. G. Huey, D. J. Tanner, F. M. Flocke, and J. M. Roberts (2004), A thermal dissociation-chemical ionization mass spectrometry (TD-CIMS) technique for the simultaneous measurement of peroxyacyl nitrates and dinitrogen pentoxide, *J. Geophys. Res.*, *109*, D19315, doi:10.1029/2004JD004670.

Trainer, M., B. A. Ridley, M. P. Buhr, G. Kok, J. Walega, G. Hubler, D. D. Parrish, and F. C. Fehsenfeld (1995), Regional ozone and urban plumes in the southeastern United-States - Birmingham, a case-study, *J. Geophys. Res.*, *100*(D9), 18,823–18,834, doi:10.1029/95JD01641.

U. S. Census Bureau (2006), *Annual Estimates of the Population of Metropolitan and Micropolitan Statistical Areas: April 1, 2000 to July 1, 2007 (CBSA-EST2007-01)*, edited by U. S. Census Bureau.

Warneke, C., et al. (2010), Biogenic emission measurement and inventories determination of biogenic emissions in the eastern United States and Texas and comparison with biogenic emission inventories, *J. Geophys. Res.*, *115*, D00F18, doi:10.1029/2002JD012445.

Weibring, P., D. Richter, J. G. Walega, and A. Fried (2007), First demonstration of a high performance difference frequency spectrometer on airborne platforms, *Opt. Exp.*, *15*(21), 13,476–13,495.

Wert, B. P., et al. (2003), Signatures of terminal alkene oxidation in airborne formaldehyde measurements during TexAQS 2000, *J. Geophys. Res.*, *108*(D3), 4104, doi:10.1029/2002JD002502.

White, W. H., J. A. Anderson, D. L. Blumenthal, R. B. Husar, N. V. Gillani, J. D. Husar, and W. E. Wilson (1976), Formation and transport of secondary air-pollutants – ozone and aerosols in St. Louis urban plume, *Science*, *194*(4261), 187–189.

Wiedinmyer, C., A. Guenther, M. Estes, I. W. Strange, G. Yarwood, and D. T. Allen (2001), A land use data base and examples of biogenic isoprene emission estimates for the state of Texas, USA, *Atmos. Environ.*, *35*(36), 6465–6477.

E. L. Atlas, Division of Marine and Atmospheric Chemistry, University of Miami, 4600 Rickenbacker Causeway, Miami, FL 33149, USA.

J. A. de Gouw, G. J. Frost, J. S. Holloway, D. D. Parrish, J. Peischl, T. B. Ryerson, M. Trainer, C. Warneke, and R. A. Washenfelder, Chemical Sciences Division, Earth System Research Laboratory, National Oceanic and Atmospheric Administration, 325 Broadway, Boulder, CO 80305, USA. (rebecca.washenfelder@noaa.gov)

F. M. Flocke, A. Fried, D. Richter, S. M. Schauffler, J. G. Walega, P. Weibring, and W. Zheng, Earth Observing Laboratory, National Center for Atmospheric Research, P.O. Box 3000, Boulder, CO 80307, USA.